Available online at www.sciencedirect.com
SCIENCE DIRECT®
Organic Electronics 4 (2003) 89–103
Organic Electronics
www.elsevier.com/locate/orgel

Doped organic semiconductors: Physics and application in light emitting diodes

M. Pfeiffer [a,*], K. Leo [a], X. Zhou [a], J.S. Huang [a], M. Hofmann [a], A. Werner [a], J. Blochwitz-Nimoth [b]

[a] *Institut für Angewandte Photophysik, Technische Universität Dresden, D-01062 Dresden, Germany*
[b] *Novaled GmbH, Zellescher Weg 17, 01069 Dresden, Germany*

Abstract

In this paper, we discuss recent experiments which prove that evaporated organic films can be efficiently doped by co-evaporation with organic dopant molecules. Key advantages for devices are the high conductivity and the formation of ohmic contacts despite large energetic barriers. For p-type doping, efficient doping is possible for a variety of poly-crystalline and amorphous materials. Despite the differences in the microscopic behavior, all basic effects known from doped inorganic semiconductors are found in organics as well. However, efficient n-type doping with stable molecular dopants is still a challenge.

Organic light emitting diodes (OLED) with conductivity doped transport layers show significantly improved properties: For instance, we have achieved a brightness of 100 cd/m^2 already at a voltage of 2.55 V, well below previous results for undoped devices. The advantages of doping are even more pronounced for top-emitting, inverted OLED structures: Due to the ohmic contacts nearly independent of the contact properties, it is possible to realize inverted top-emitting devices with parameters comparable to standard devices. Our doping technology is thus a significant advantage for active-matrix OLED displays and other displays on opaque substrate.

PACS: 72.80.Le; 78.60.Fi
Keywords: OLED; Doping; Conductivity; Charge injection; Low voltage; High efficiency

1. Introduction

The large majority of present-day devices based on semiconductors are using inorganic crystalline materials, with single-crystalline silicon dominating by about a factor of 1000 compared to other materials like GaAs. Despite the advantages of single-crystalline inorganic semiconductors like high mobility (on the order of 100 to 1000 cm^2/Vs) and high stability, these materials are less suitable if applications require low cost and large area. As an alternative, amorphous inorganic semiconductors have been developed, with a breakthrough in the 1970s when Spear and Le Comber developed hydrogenated amorphous silicon which could by n- and p-type doped [1]. Despite their low mobilities (on the order of 1 cm^2/Vs), they are broadly applied, e.g., for low-cost solar cells.

* Corresponding author: Tel.: +49-351-46337559; fax: +49-351-46337065.
E-mail address: pfeiffer@iapp.de (M. Pfeiffer).

1566-1199/$ - see front matter © 2003 Elsevier B.V. All rights reserved.
doi:10.1016/j.orgel.2003.08.004

As an alternative to inorganic semiconductors, organic materials have recently gained much attention (for a review, see [2]). Originally, much of the research has concentrated on single crystals, which can show mobilites of a few cm^2/Vs at room temperature and even much higher values at low temperature, as shown in the pioneering work of Karl [3]. However, for practical applications as thin films, organic semiconductors with disordered structures, such as evaporated small-molecule materials of polymers processed from solution are prevailing. In photoconductors for copiers and laser printers, organic semiconductors are already broadly applied.

Organic semiconductors have unique physical properties, which offer many advantages to inorganic semiconductors: (i) The extremely high absorption coefficients in the visible range of some dyes offer the possibility to prepare very thin photodetectors and photovoltaic cells [4]. Due to the small thickness of the layers, the requirements on chemical and structural perfection are reduced since the excitation energy does not have to travel long ways. (ii) Many fluorescent dyes emit strongly red shifted to their absorption. Thus, there are almost no reabsorption losses in organic light emitting diodes (OLEDs) [5], which, together with the low indices of refraction, circumvents the key problems of inorganic LED. (iii) Since organic semiconductors consist of molecular structures with saturated electron systems, the number of intrinsic defects in disordered systems is much lower than in inorganic amorphous semiconductors, where a large number of dangling bonds exist. (iv) There is a nearly unlimited number of chemical compounds available, and it is possible to tailor materials.

It is worthwhile to remind that the breakthrough of the classical silicon technology came in the very moment the conduction type was no longer determined by impurities but could be controlled by doping. Unlike inorganic semiconductors, up to now, organic dyes are usually prepared in a nominally undoped form. However, controlled and stable doping is a prerequisite for the realization and the efficiency of many organic-based devices. If we succeed in shifting the Fermi level towards the transport states, this could reduce ohmic losses, ease carrier injection from contacts and increase the built-in potential of Schottky- or pn-junctions.

Here, we review our recent work on doping of organic semiconductors. In particular, we have concentrated on evaporated layers which were doped by coevaporation with a molecular dopant. The paper is organized as follows. First, we discuss the basic physics of doping, both for p-type and n-type model materials. Then, we discuss the application of conductivity [1] doped organic layers in OLED devices. Finally, we conclude with an outlook to future challenges and opportunities for conductivity-doping of organics. For experimental details, the reader is refered to the references cited for the various sample structures and characterization techniques.

2. Doping fundamentals

The basic principle of doping in organic semiconductors is similar to that in inorganic materials: one has to add impurities which either transfer and electron to the electron conducting (LUMO) states (n-type doping) or remove an electron from the hole conducting (HOMO) states to generate a free hole.

It has been shown that very high conductivities can be achieved when organic dyes with a weak donor character like the phthalocyanines are exposed to strongly oxidizing gases like iodine or bromine [6]. However, such small dopants can easily diffuse in the layers, so this technique is not suitable to prepare thermally stable bipolar devices such as pn- or pin-junctions. Similar considerations hold for doping by other small atoms like Lithium [7] or small molecules like Lewis acids [8].

A better pathway to conductivity-doping for stable devices is to use larger aromatic molecules being strong π-electron donors or acceptors. There have been scattered results on molecular doping in the last decades.

[1] We refer to p- and n-doping as *conductivity-doping* to avoid confusion with the admixture of emissive dyes to a matrix material which is also often denoted as doping in the OLED community. We prefer the term *conductivity-doping* because the term *electrical doping* might suggest that doping is done by electrical means (compare *electrochemical doping*).

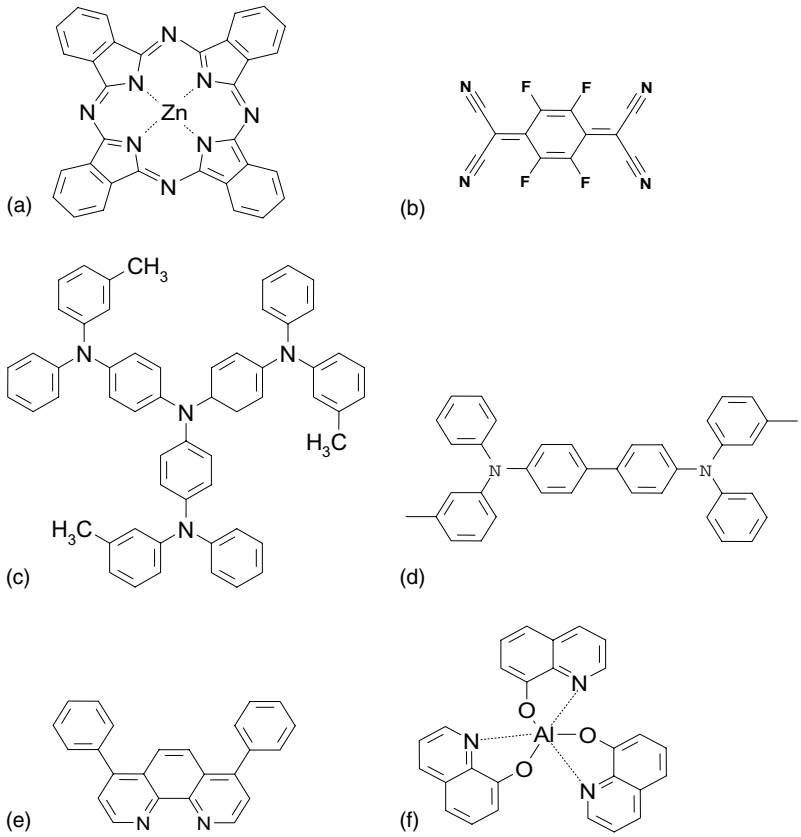

Fig. 1. Chemical structures of some prototype materials mention in this report (a) zinc phthalocyanine (ZnPc), a low gap hole transport material that forms polycrystalloine layers (b) 2,3,56-tetrafluoro-7,7,8,8-tetracyano-quinodimethane (F_4-TCNQ), a strong π-electron acceptor (c) tris-(phenyl-3-methyl-phenyl-amine)-triphenylamine (m-MTDATA), an amorphous wide gap hole transport material (d) aluminium-tris-8-hydroxy-quinoline (Alq_3), an electron transport and green emitter material (f) batho-phenanthroline (BPhen), a wide gap electron transport material used for hole blocking layers because of its high ionization energy.

For instance, phthalocyanines have been doped by adding organic acceptor molecules like *ortho*-chloranil [9], tetracyno-quinodimethane (TCNQ) or dicyano-dichloro-quinone (DDQ) [10,11]. Covalently bonded stack phthalocyanines [12] and oligothiophenes [13] have been doped by DDQ. However, systematic investigations into the influence of doping on fundamental semiconductor parameters like the Fermi level or the carrier density are still rare. A proper thermodynamic description of the doping process is still a challenge. Apart from that, only a few attempts have been described in the literature to apply molecularly doped dye layers in semiconductor devices [10,13].

In the following, we first discuss our approach to doping by coevaporation of dopants with the organic matrix. We first discuss p-type doping, where we have performed extensive investigations with both polycristalline and amorphous matrix materials, and then briefly touch the issue of n-type doping. The chemical structures for some typical molcules mentioned in this report are shown in Fig. 1.

2.1. p-Type doping

In the last few years, we have systematically studied the physics of molecular doping of organics [14–17] and have successfully applied

conductivity doped transport layers to both OLEDs [18–22] and solar cells [23,24]. First, we have mainly addressed phthalocyanines as model systems for p-type doping.

Fig. 2 shows the conductitivity of ZnPc doped with the strong electron acceptor F_4-TCNQ as a function of the molecular doping ratio. It is obvious that the conductivity can be reproducibly controlled over more than two orders of magnitude by the doping ratio; furthermore, the conductivitity is many orders of magnitude higher than the background conductivity of nominally undoped ZnPc (10^{-10} S/cm in vacuo). The dashed line in Fig. 1 shows that the conductivity rises much faster than linearly with the doping ratio, which is explained within a percolation model by a subtle interplay between charge carrier release by doping and a filling of a distribution of more or less localized states [17].

To further understand the electrical properties of the doped layers, we have performed measurements of the thermoelectric effect (Seebeck effect) [14,17]. The Seebeck effect is a useful and simple tool to measure the distance between the transport states (which we denote E_μ here) and the Fermi level E_F. In a simple analysis, it turns out that the Seebeck coefficient $S(T)$, being the relation between thermovoltage and temperature difference between the contacts, can be written as

$$S(T) = \frac{1}{e}\left(\frac{E_F - E_\mu}{T}\right) + A$$

where e is the elementary charge, T the absolute temperature and A is a numerical factor which accounts for the kinetic energy of the charge carriers and is therefore assumed to be negligible in organic low mobility narrow gap materials [25].

Fig. 3 shows the position of the Fermi level in ZnPc as a function of temperature and molecular doping concentration. It is obvious that the Fermi level shows the typical behavior for a doped semiconductor: With increasing doping, the Fermi level moves towards the transport states; with increasing temperature, it moves towards the center of the band gap. These conclusions still hold in the framework of a more elaborate percolation model [17], even if such model implies that not only the Fermi level, but also the dominant transport level E_μ slightly moves with temperature and doping level.

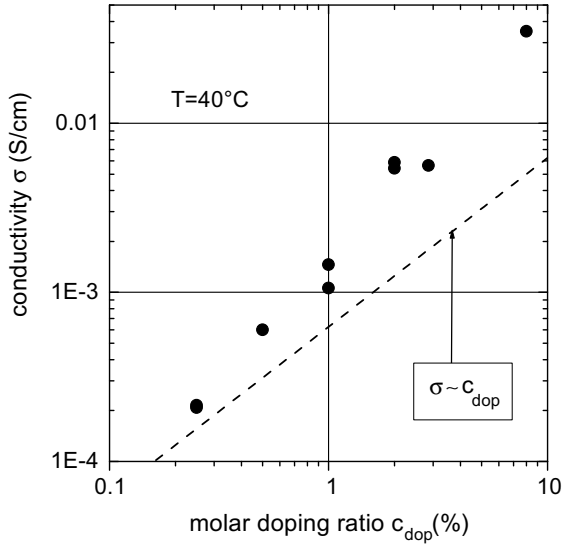

Fig. 2. Conductivity of p-doped zinc phthalocaynine as a function of the doping concentration with the molecular dopant F_4-TCNQ, measured in a coplanar contact geometry on a fused silica substrate (cf. [17]).

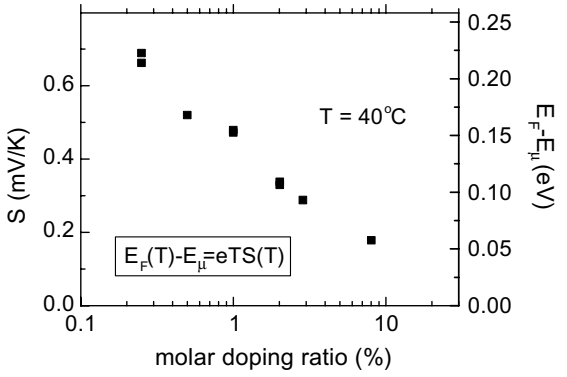

Fig. 3. Seebeck coefficient S (left axis) and distance between the Fermi energy level E_F and the dominant transport energylevel E_μ (right axis) at 40 °C, calculated according to the formula given in the inset, for ZnPc layers doped with F_4-TCNQ as a function of the doping concentration. The Fermi level behaves in close agreement with inorganic semiconductors; i.e., it moves to the transport state with increasing doping concentration and moves towards the center of the gap for increasing temperature. For experimental details see [14,50].

Table 1
p-doping of various hole transport materials by TCNQ derivatives: The table shows the solid state ionization energy I_s of the matrix materials, the degree of charge transfer from the matrix to the dopant, derived from the position of the $b_{1u}\nu_{18}$ mode of the TCNQ derivatives and the conductivity at a doping level of 2 mol% for a series of matrix/dopant combinations

Matrix/Dopant	ZnPc/F_4-TCNQ	ZnPc/TCNQ	m-MTDATA/F_4-TCNQ	TPD/F_4-TCNQ	MeO-TPD/F_4-TCNQ
I_s (eV)	5.1 [49]	5.1	5.1 [50]	5.4 [28]	–
Z	1	1	1	0.64	0.74
σ (S/cm)	1×10^{-3}	1×10^{-6}	3×10^{-7}	1×10^{-7}	1×10^{-5}

We have investigated the p-type doping using F_4-TCNQ with a variety of hole transport matrices. It turned out that the doping is a general effect that works for a large number of materials. For application of doped layers in optoelectronic devices like OLEDs and solar cells, it is especially important that amorphous wide gap hole transport materials such as TDATA (4,4′,4″-tris-*N*,*N*-diphenyl-amino-triphenylamine) [26] can be doped as well. The resulting conductivities are in the order of 1×10^{-7} to 1×10^{-5} S/cm at a doping level of 2% F_4-TCNQ. The reason for the much lower conductivity as compared to the polycrystalline phthalocyanine as shown in Fig. 1 is the stronger localization of the charge carriers in the amorphous material [17]; the carrier concentrations are comparable. [2]

Using infrared spectroscopy, it is possible to follow the charge transfer from the matrix molecules to the acceptor dopant [15]: The exact position of the streching mode of the C–N triple bond in the cyano groups of F_4-TCNQ is sensitive to its charge state und thus provides direct information on the degree of charge transfer Z. The results for a number of materials are listed in Table 1. A complete charge transfer ($Z = 1$) is found for matrix materials like the phthalocyanines and TDATA derivatives like m-MTDATA. They have ionization energies around 5 eV which is close to the electron affinity of F_4-TCNQ [15,27]. Using TCNQ instead of F_4-TCNQ as a dopant, the degree of charge transfer is low even in ZnPc ($Z = 0.2$) and consequently the conductivity at 2% doping is only in the order of 1×10^{-6} S/cm for TCNQ instead of 1×10^{-3} S/cm for F_4-TCNQ in ZnPc. Here, it becomes obvious that only the enhancement of electron affinity by about 0.5 eV by fluorination of TCNQ enabled us to achieve an efficient molecular doping [14].

On the other hand, we observe an only partial charge transfer for F_4-TCNQ in TPD ($Z = 0.64$) due to its ionization energy of around 5.4 eV [28] being about 0.4 eV higher than e.g. for m-MTDATA [29]. Accordingly, the conductivity for a given doping ratio of 2 mol% is lower for TPD (1×10^{-7} S/cm) than for m-MTDATA (3×10^{-7} S/cm) even though the hole mobility in m-MTDATA (3×10^{-5} cm^2/Vs [29]) is more than one order of magnitude lower than in TPD (1×10^{-3} cm^2/Vs [30]). By attaching one electron pushing methoxy group to each of the four outer benzene rings of TPD, its ionization energy can be reduced. This material (MeOTPD) seems to have similarly high hole mobility as TPD, but a higher degree of charge transfer ($Z = 0.73$) and thus yields the highest conductivity (5×10^{-6} S/cm at 2% doping) among the amorphous hole transport materials we have tested so far.

Obviously, the conductivity is very sensitive to minor differences in Z. Here, it should be noted that Z is not a probability for a complete charge transfer, but rather has to be understood in terms of mixing coefficients for an orbital being a linear combination of the acceptor LUMO and the matrix HOMO.

2.2. n-Type doping

In contrast to p-type doping, n-type molecular doping is intrinsically more difficult due to the following fact: For efficient doping, the HOMO

[2] For the highest doping concentrations (a few percent of dopants), they are around 10^{19} to 10^{20} cm^{-3}. However, in organic materials, such doping levels still lead to semiconducting properties due to the high density of states in the LUMO level and the weak coupling of the dopant energy levels.

level of the dopant must be energetically above the LUMO level of the matrix material, which makes such materials unstable against oxygen. For materials with low-lying LUMO level, i.e. high electron affinity, we have achieved reasonable conductivities using the dopant BEDT-TTF [16]. This approach, however, does not work for typical OLED electron transporting materials which have a rather low electron affinity on the order of 3 eV.

An alternative approach is the use of alkali metals like Li or Cs [31]. In contrast to molecular doping, where dopant concentrations of a few percentage are sufficient, one needs for alkali metals levels up to 1:1 molecule/dopant atom. Also, the stability of the doping with alkali metals under device operation is an issue which is not entirely solved.

Recently, we have developed a novel doping method using salts of cationic dyes like rhodamoine B as stable precursors for strong molecular donors [32]. The method has already been successfully applied for solar cells [24], where materials with lower lying LUMO are used. For OLEDs, development of suitable molecular dopants is under way.

3. OLED with doped transport layers

3.1. Basic effects of doping in OLED devices

First, we dicuss the importance of doping for OLED devices: Why is it useful to use doped transport layers in an OLED? Fig. 4 shows a schematic comparison of a classical III–V LED (a) and an organic LED without doping (b). The inorganic semiconductor device is a p–i–n structure, consisting of two highly doped transport layers for electrons and holes and a nominally undoped or weakly doped emitter layer with smaller band gap. The use of the highly doped transport layers has two key advantages: First, due to the high conductivity, the electric field in the doped transport layers is quite low. Thus, the device operates close to flat band condition. The current–voltage relationship is determined by the pn-heterojunction (and not by space charge limited current injection into the transport layers) and has therefore exponential characteristics. The operating voltage V of the device is close to the photon energy $eV = hv$, i.e. for a green device, $V \cong 2.5$ V even for high brightness.

In the organic device, on the other hand, one needs to inject the carriers from the contact, leading to space charge limited currents where the current–voltage characteristics follow a power law. Thus, devices with undoped transport layers typically have less steep characteristics, which is a disadvantage for many applications, e.g., passive matrix displays. Also, there are high fields in the device under operation, requiring excessive operating voltage to achieve high brightness. The excessive voltage is dissipated in the device, causing additional heat.

A second, possibly even more important advantage of a doped device are the contact pro-

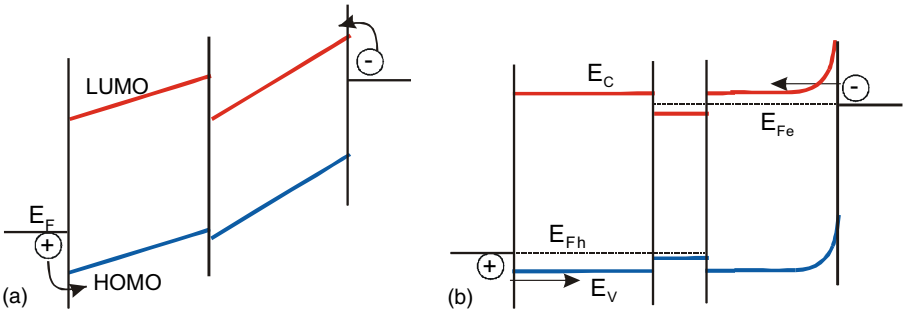

Fig. 4. Schematic energy diagrams under operation bias of (a) a two-layer OLED with undoped transport layers and (b) of a typical p–i–n structure realized e.g. in III–V semiconductor LEDs. E_{Fe} and E_{Fh} denote the quasi Fermi levels for electrons and holes, which align between the contacts and the respective doped transport layers in the p–i–n structure.

perties: As schematically shown for the pin-device (a), the ohmic contacts are usually formed by a highly doped layer at the interface. The thin barrier formed by this space charge layer allows ohmic injection despite the existence of considerable energy barriers between the transport level of the semiconductor and the work function of the contact metal: The carriers can tunnel through the thin barrier which is formed.

In contrast, in the undoped device (b), the carriers need to overcome the barrier. Thus, undoped OLEDs are usually very sensitive to the electronic properties of the contact materials. Typically, the ITO has to be specially treated to adjust the work function [33]; on the cathode side, low work function metals or specific interlayers have to be used. These problems are critical if the OLED devices should be realized on substrates where the work function is not well aligned to the organic layers or cannot be easily controlled by processing steps.

3.2. Contacts with doped semiconductors

As argued above, doping leads to higher conductivities which reduce the operating voltages of devices due to lower fields in the transport region. A second effect which is important for devices has been outlined in the comparison with inorganic LED devices in the previous section: When ohmic contacts with metals (or highly doped transparent oxides, as frequently used in OLED) are realized, the energetic alignment at the contact plays a crucial role. Ideally, one would choose the contact materials in a way that the work function of the metals or conductive oxides aligns well with the LUMO level at the electron injecting contact and with the HOMO at the hole injecting contact.

However, due to constraints in the materials choice, this is rarely possible. For instance, the typical OLED electron transporting materials have electron affinities around 3 eV, which would require very reactive materials for ohmic contacts. On the anode side, the typical conductive oxides have work functions which are energetically too high for hole injection. In most contact systems for inorganic semiconductors, these problems are solved by introduction of highly doped space charge layers. Many contact materials for inorganic devices are compounds consisting of a noble metal with an admixture of another metal which produces a doping effect. After deposition, the contacts are then annealed at a temperature where the admixture diffuses into the semiconductor and forms a highly doped space region. This region leads to a thin barrier where the carriers can easily tunnel through.

We have recently shown in a spectroscopic study that there is an exactly corresponding effect for contacts to organic semiconductors [49]. The experiments used X-ray and ultraviolet photoemission to study the energetic levels of contact materials and organic semiconductors close to the interface. As model system for the organic semiconductor, zinc phthalocyanine and F_4-TCNQ was chosen. As substrates, both ITO and polycrystalline gold were used. The organic layers where evaporated in steps on the substrates; after each step, spectra were taken to follow the energy levels as a function of the thickness of the organic layers. The work function and the HOMO levels were determined using well established methods of photoelectron spectroscopy [49].

Fig. 5 shows the results for nominally undoped ZnPc (left) and 1:30 doped ZnPc (right) on an ITO substrate. In both cases, a rather large energy barrier for holes of about 1.2 eV is visible; also, both cases show a small interface dipole which is probably caused by a local charge transfer at the interface. For the undoped samples, there is a weak level bending observable in the organic semiconductor before the level becomes flat for thicknesses above 15 nm. In the bulk, the HOMO level of the ZnPc is about 0.8 eV away from the Fermi level, which is consistent with an undoped semiconductor where the Fermi level is in the band gap center.

For the doped semiconductor, there is a much stronger level bending of 0.9 eV. The Fermi level is now only 0.23 eV away from the HOMO level, which is consistent with the data presented in Section 2.1. The space charge layer is now very thin, below the experimental resolution of 5 nm. A calculation using the Poisson equation yields 2.5 nm.

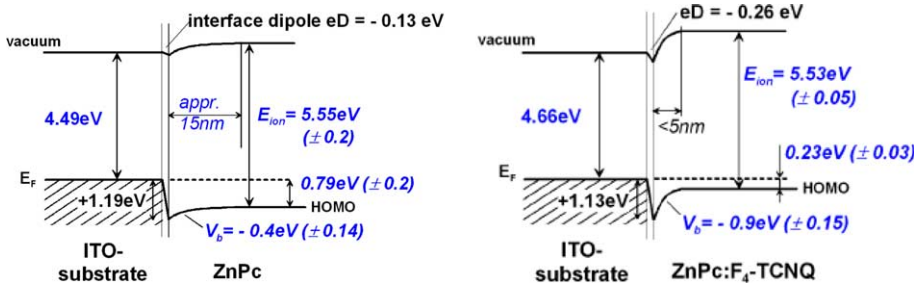

Fig. 5. Energy diagram as derived from UPS/XPS spectroscopy showing the vacuum level, the HOMO onset and the Fermi level E_F for the organic semiconductor ZnPc on ITO. Left side: undoped ZnPc on ITO; right side: ZnPc doped with F_4-TCNQ [49].

The electrical properties of such contacts are in good agreement with these findings: Undoped phthalocyanines on ITO form blocking contacts, as is expected for the energetic alignment in Fig. 5 left side. Contacts with doped phthalocyanines, however, are ohmic despite the rather large barrier. One can thus conclude that the basic mechanism of forming an ohmic contact by providing an extremely thin barrier works as well as in inorganic semiconductors.

This effect of doping on the injection behavior is demonstrated in Fig. 6 for two samples based on m-MTDATA, a typical hole transport material for OLEDs. As opposed to ZnPc, it has the advantage of forming very smooth layers so that undoped interlayers of well defined thickness can be realized. The samples have the layer sequence ITO/m-MTDATA (undoped, thickness w)/m-MTDATA (p-doped with 2% F_4-TCNQ, 100 nm)/Au.

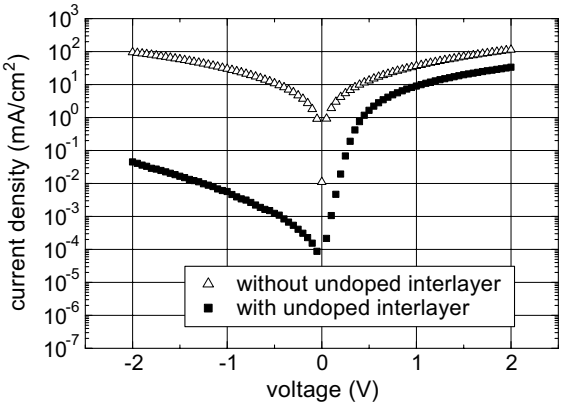

Fig. 6. Current–voltage characteristics for junctions between ITO and p-doped m-MTDATA (100 nm, doped with 2 mol% F_4-TCNQ), with and without an undoped interlayer of 50 nm undoped m-MTDATA. Gold is used as a nearly Ohmic contact to the p-doped layer.

Here, the gold top contact is nearly ohmic while there is a considerable injection barrier for holes from ITO to m-MTDATA. Accordingly, devices with an undoped interlayer ($w > 0$) behave as Mip-type diodes (cf. [34]), having a built-in field due to Fermi level adjustment between the ITO and the doped m-MTDATA across the undoped interlayer. While the forward currents of these diodes are only weakly affected by the thickness w of the undoped interlayer, currents at reverse bias increase systematically with decreasing w. With $w = 50$ nm, we observe a rather high rectification ratio in excess of 1000:1 at ±1 V. The barrier for hole injection from ITO into m-MTDATA is obviously high using untreated ITO. On the other hand, the device without undoped interlayer has basically symmetric IV characteristics demonstrating easy hole injection from ITO into doped m-MTDATA. This may be by tunneling or similar processes like field assisted hopping between gap states that are favored by the fact that the thickness of the barrier becomes extremely low with high doping levels.

3.3. Efficient OLEDs with doped transport layers

As a first step, one could try to realize doped OLED devices using the same approach inorganic devices suggest; i.e., realize a simple p–i–n structure. As it turns out, this leads to devices with low operating voltage, but also low efficiencies. This

was particularly pronounced with our first attempts which used phthalocyanines for the hole transport layer (HTL), which are also not well suited due to their electronic properties [18].

In the following, we first discuss the effect of a p-type HTL on the properties of OLED devices. Then, we discuss how an undoped blocking layer between the doped transport layer and the emitter layer drastically enhances the efficiency of the devices.

3.3.1. Influence of doping on the device

Fig. 7(a) shows the current–voltage curves of a series of OLED structures with the layer sequence ITO/TDATA(200 nm)/Alq_3(65 nm)/LiF(1 nm)/Al. The data show that the currents for the doped samples for a given voltage are much higher than for the undoped structure. This finding is in agreement with the conclusion from the last section that the doped HTL is very efficient in improving the carrier injection into the transport layer. Again, the very low currents for the undoped device are due to the fact that the ITO has not been treated by oxygen plasma or ozone to increase its work function. Fig. 7(b) shows the luminance–voltage curves of the samples. Due to the much higher currents, the sample with doped transport layers reaches higher luminance at a given voltage. However, the current efficiency of all these samples is very low (<1 cd/A) and even decreases with increasing doping. We qualitatively explain this behavior as follows: At the interface between TDATA and Alq_3, the energetics allow the formation of interface excitons or exciplexes (cf. Fig. 8(a)). The luminescence of such interface excitons has actually been observed in experiment [35]. In our case, these interface excitons are close to a high concentration of holes. Thus, there seems to be a high probability that they recombine non-radiatively, thus leading to recombination currents in the device without generation of light at the Alq_3 emission wavelength.

The problem of the non-radiative recombination and the concomitant low efficiency of the OLED devices can be solved by the introduction of a suitable undoped interlayer (Fig. 8(b)), as we discuss in the next section.

3.3.2. Influence of blocking layer

To achieve low operating voltage and high efficiency, it is necessary to prevent the formation and non-radiative recombination of interface excitons. We have shown that it is possible to solve this problem by the insertion of a thin undoped interlayer of a suitable material [19]. The energetic arrangement of all materials in the layer system needs to be carefully chosen (see Fig. 8): (i) The LUMO of the undoped buffer must be considerably higher than for the emission layer (EML) to make sure that electrons cannot penetrate into the HTL. We will therefore denote this buffer as an electron blocking layer (EBL). (ii) The barrier for hole injection from the EBL into the EML should be small enough to make sure that the energy of a charge carrier pair consisting of a hole on the EBL and an electron on a neighboring molecule of the

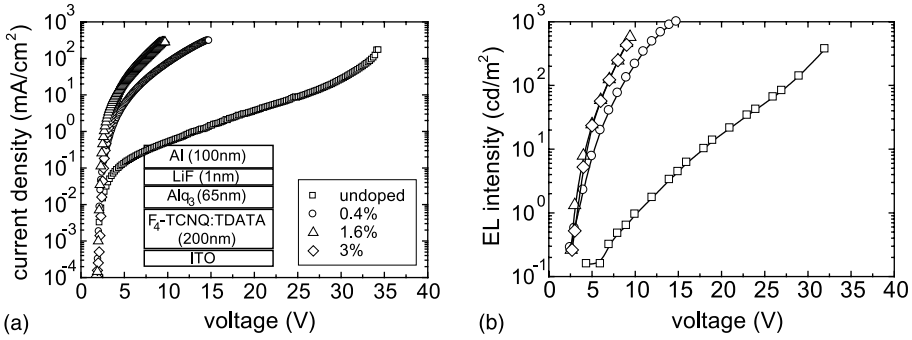

Fig. 7. Current–voltage and luminance–voltage characteristics for a series of OLEDs with the layer sequence ITO/TDATA (200 nm, doped with various concentrations of F_4-TCNQ)/Alq_3(65 nm)/LiF(1 nm)/Al [19].

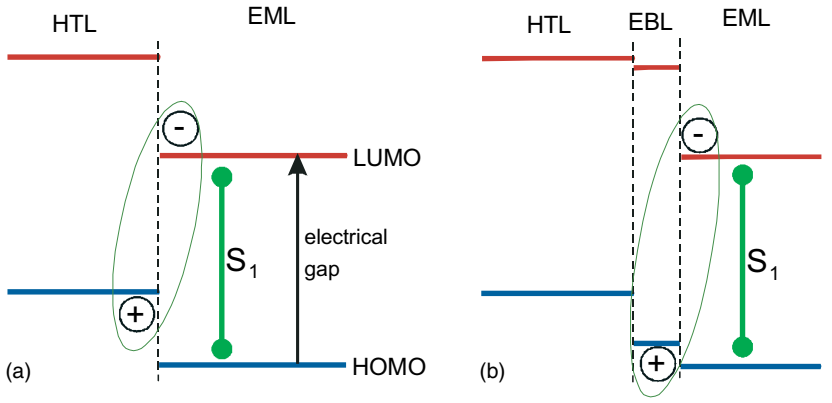

Fig. 8. Exciplex and exciton formation at a heterointerface between a HTL and an EML. (a) Due to the too high HOMO offset, the energy of an interface carrier pair is lower than the energy of a singlet excition S_1 in the EML, which favors the formation of exciplexes. (b) An interlayer (EBL) between the HTL and the EML leads to a situation where the energy of the interface carrier pair is higher than the S_1 energy in the EML. Excitons in the EML can be generated by hole transfer to a negatively charged EML molecule at the interface. In spite of the non-vanishing HOMO offset, the process can be barrier-free due to the gain in Coulomb energy, i.e. the exciton binding energy. To allow for efficient p-doping, the HOMO position of the HTL is chosen such that it is close to resonance with the LUMO of an acceptor A.

EML is higher than the lowest singlet exciton energy in the EML. Roughly spoken, this criterion means than the HOMO offset must be lower than the difference between the exciton binding energy of a singlet exciton and Coulomb binding energy of the interface carrier pair. Only in that case, interface carrier pairs can be easily transformed into Frenkel excitons on the EML. (iii) The ionization energy of the hole transport material must be low enough to allow for an efficient electron transfer to the acceptor dopants to make sure that the doped HTL has a sufficient conductivity. (iv) It is desirable for the LUMO of the HTL to be above the LUMO of the EML, i.e. not only the EBL but also the HTL should have a wide gap. In that case, electrons from the EML cannot tunnel through the EBL into the HTL and the EBL can be made as thin as 5 nm. For low gap HTL materials like phthalocyanines, however, we found that the EBL must be as thick as 20 nm to obtain the full efficiency. Finally, (v) the HOMO offset between the HTL and the EBL should not be too high to keep the driving voltage for hole injection low.

For F_4-TCNQ as an acceptor and Alq_3 as an EML material, criterion (ii) and (iii) cannot be simultaneously fulfilled using the same matrix material for the HTL and the EBL. However, it turns out to be a good choice to use m-MTDATA for the HTL because it can be efficiently doped and NPD or TPD for the EBL because its interface to Alq_3 ensures efficient exciton formation on Alq_3.

As a consequence of this energetic arrangement, there is a barrier for hole injection from the HTL into the EBL. This is to be expected according to the different ionization energies of TPD (around 5.4 eV [28]) and TDATA (around 5.1 eV [50]). This barrier is also obvious from the series of samples with different thicknesses of the TPD interlayer between doped TDATA and Alq_3 shown in Fig. 9: The IV characteristics are extremely sensitive to the thickness of TPD. The voltage, e.g., to reach a current level of 10 mA/cm^2 is increased from 4.5 to 7 V when the TPD thickness is changed from 5 to 20 nm. This strong influence cannot be explained in terms of space charge limited currents in TPD [36], as TPD has a quite high hole mobility [30]. It is thus a clear indication for field dependent injection. One might think that this is a drawback for steep IV-characteristics. However, in the final analysis, it turns out that it is even the ideal situation for Alq_3 based devices: It has been found that the efficiency of such OLEDs goes down if the hole injection is too efficient. Obviously, accumulated positive charges close to the

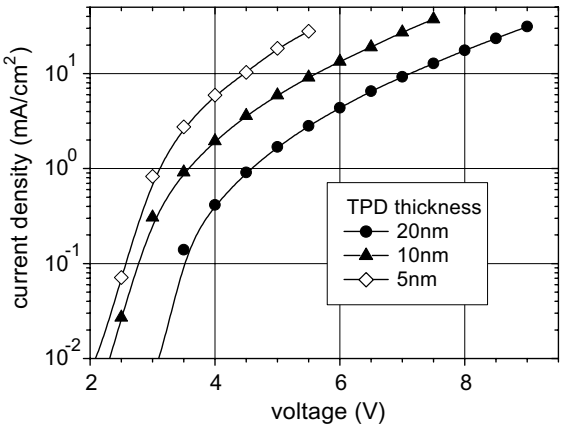

Fig. 9. Current–voltage characteristics for a series of OLEDs with the layer sequence ITO/TDATA (100 nm, doped with 2 mol% F_4-TCNQ)/TPD(varying thickness)/Alq3(65 nm)/LiF(0.5 nm)/Al.

NPD/Alq_3 interface (cf. [37] and Fig. 10) lead to a partial quenching of luminescence. What is more, a surplus of holes at the interface increases the probability that Alq_3 cations are formed, which are known to be unstable [38] and lead to rapid device degradation. Accordingly, the efficiency and lifetime can be improved on the expense of an increased operating voltage by making the hole injection into the HTL more difficult, e.g. by introducing an interlayer of CuPc [39]. However, the combination of a doped HTL and a thin EBL with an energetic barrier in between leads to the following scenario: The positive charge is rather accumulated at the HTL/EBL interface than at the EBL/EML interface (Fig. 10). Accordingly, the efficiency is high. At the same time, the operating voltage is low because the EBL can be extremely thin. A direct comparison of OLEDs with 60 nm Alq_3 as an EML and (A) 50 nm of NPD [5] and (B) 50 nm doped m-MTDATA and 6 nm NPD [19] as a HTL system, prepared and characterized under identical conditions, confirms this idea [40]. With optimum treatment of ITO, the two types of devices have very similar operating voltage. However, the efficiency of type B devices is systematically and reproducibly higher by about 30%.

3.3.3. OLEDs with conductivity-doping and emitter doping

One question one might ask is whether the concept of doped transport layers is compatible for all kinds of emitter layers. It is well known that the efficiency of Alq_3 based OLEDs can be significantly enhanced by admixture of a small concentration (0.5–2%) of laser dyes such as quinacridone (QAD) [41] or coumarine derivatives [42,43]. Indeed, we found an increased efficiency using Alq_3:QAD (100:1) as an EML in OLEDs with p-doped HTL. At the same time, however, the driving voltage becomes significantly higher by the QAD admixture if the same EML thickness is used. As the main recombination region is very

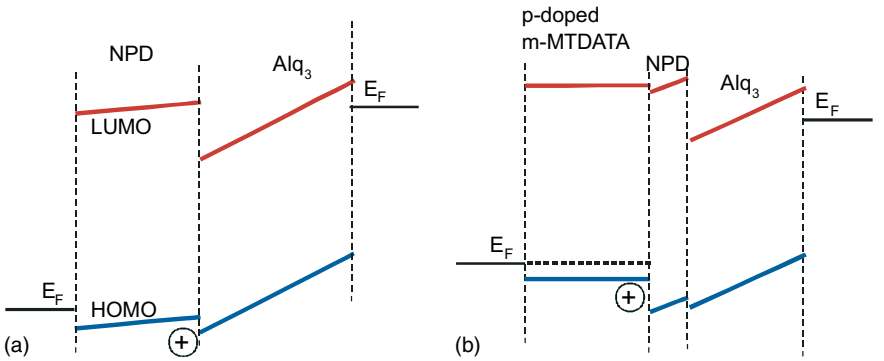

Fig. 10. Proposed energy level schemes for (a) a typical two-layer OLED and (b) an OLED with doped HTL, buffer layer and EML as proposed by Zhou et al. [19]. According to Poisson's equation, the kink in the potentials close to the NPD/Alq_3 interface in (a) corresponds to a positive space charge. In (b), the positive space charge is rather at the m-MTDATA/NPD interface where it does not affect the quantum efficiency or the lifetime of the device.

close to the HTL/ETL interface in Alq_3 based devices [36], the increased driving voltage can only be explained by a decrease in effective *electron* mobility. Obviously, QAD forms electron traps in Alq_3. Nevertheless, low voltage devices could be realized by reducing both the total thickness of the Alq_3 layer and the thickness of the QAD doped region close to the interface. As shown in Fig. 11, a device with the layer sequence ITO/TDATA(p-doped, 100 nm)/TPD(5 nm)/Alq_3:QAD(100:1, 15 nm)/Alq_3(30 nm)/LiF(1 nm)/Al shows a constantly high efficiency of 10 cd/A and reaches 100 cd/m^2 at 3.4 V [22]. More recently, we have achieved current efficiencies up to about 40 cd/A with a phosphorescent emitter structure [44] and a doped HTL system. It is thus obvious that the concept of doped transport layers is compatible with emitters of very high quantum efficiency.

3.3.4. pin-Devices

Based on the discussion in the previous sections, we can now proceed to the "ideal" p–i–n structure devices as discussed above. The three steps to achieve such a device are to realize a p-type doped HTL, an n-type doped ETL, and suitable blocking layers on both sides of the emitter layer.

Finally, we have realized a five layer p–i–n device consisting of two doped transport layers, two undoped blocking layers, and an emitter layer [20]. This device displays excellent current–voltage curves with exponential behavior up to current densities of a few tens of mA/cm^2. The luminance–voltage curve (Fig. 12) is exponential, as well, up to a brightness of about 1000 cd/m^2. The brightness of 100 cd/m^2 is reached at 2.55 V which is approximately corresponding to the energy of the green photons emitted from this device. The peak current efficiency is more than 5 cd/m^2 which is among the best values reported for devices using Alq_3 as an emitter.

In collaboration with the Princeton group (Forrest), the p–i–n architecture has been extended to phophorescent OLEDs. Using CBP:$Ir(ppy)_3$ as an emitter system, green electrophosphorescent OLEDs with extremely low operating voltages and high quantum efficiency are demonstrated [45]. These p–i–n type devices attain a brightness of 1000 cd/m^2 at only 3 V, with an external quantum efficiency of 9% and a power efficiency of 28 lm/W. At 4.0 V, 10 cd/m^2, the external quantum efficiency is 7% and the luminous power efficiency is 22 lm/W.

For these p–i–n devices, we have observed for the first time bright electrophosphorescence (100 cd/m^2) at driving voltages (2.6 V) close to the equivalent of the photon energy (2.4 eV, corresponding to the triplet energy in $Ir(ppy)_3$). This is

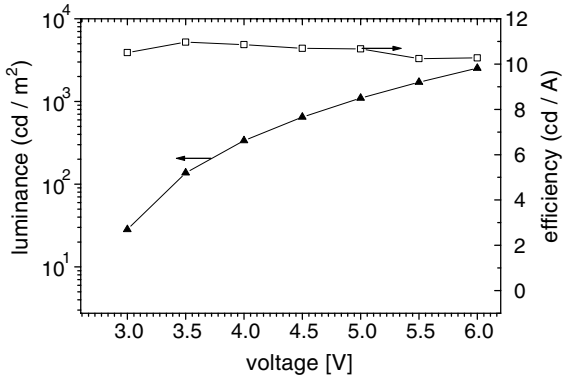

Fig. 11. Luminance–voltage characteristics (triangles) and efficiency–voltage characteristics (open squares) for an OLED with the layer sequence ITO/TDATA (100 nm, doped with 2 mol% F_4-TCNQ)/TPD(5 nm)/Alq_3:QAD(15 nm, 100:1 mixture)/Alq_3(30 nm)/LiF(1 nm)/Al(100 nm) [22].

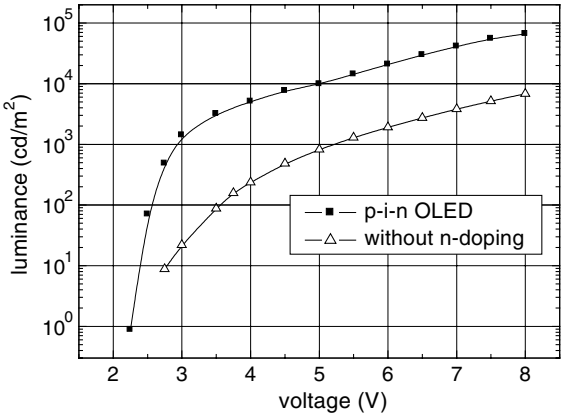

Fig. 12. Luminance–voltage characteristics of a p–i–n substrate emitting structure with the layer sequence ITO/m-MTDATA(100 nm, p-doped)/TPD(5 nm)/Alq_3(20 nm)/BPhen(10 nm)/BPhen:Li(30 nm, 1:1)/LiF(1 nm)/Al(100 nm) and an identical structure without Li-doping of the BPhen layer [20].

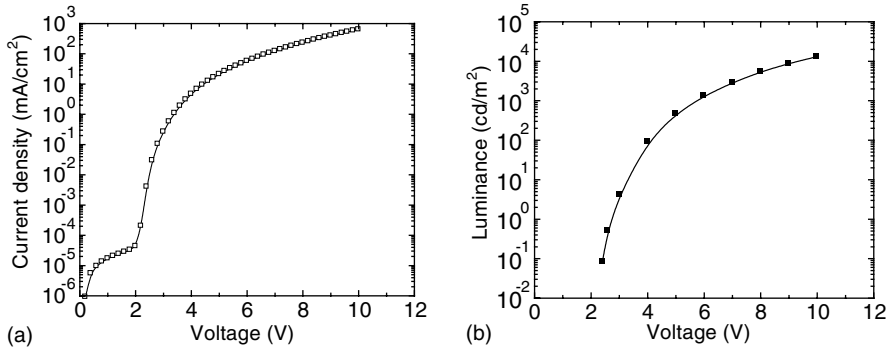

Fig. 13. Current–voltage curve of a n–i–p-type inverted top and bottom emitting device with the layer sequence ITO/BPhen:Li(15 nm)/BPhen(5 nm)/Alq_3(20 nm)/TPD(5 nm)/m-MTDATA(100 nm, p-doped)/Au [21].

a remarkable fact, as the generation of a triplet exciton from a pair of free carriers should involve a substantial energy loss. The $Ir(ppy)_3$ singlet energy is around 3 eV (estimated from the absorption edge) which implies that the energy of a free electron–hole-pair, i.e. the electrical gap of $Ir(ppy)_3$ is at least 3.5 eV. Therefore, the bright electroluminescence at 2.6 V is a strong hint that the electroluminescence process must involve a direct generation of triplet excitons on a material A, e.g. $Ir(ppy)_3$, from a hole on A and an electron on a different material B. [3] Only in that case, the energy of an injected pair of free carriers can be more or less in resonance with the triplet exciton energy. On the other hand, these results being close to thermodynamic limits prove that doping enables us to prepare optimized devices with very low transport and injection losses at brightness levels on the order of 100 cd/m^2. Only for higher brightness, where the IV-characteristics differ significantly from the exponential behavior, transport losses begin to play a significant role.

[3] In principle, electroluminescence can also occur for applied voltages below the equivalent of the gap of the emission layer, which leads to a cooling of the sample. However, a rough estimation of the current that is to be expected at 2.6 V in an organic p–n junction made of a semiconductor with 3.5 eV gap leads to a strong contradiction to the current and emission observed in the device.

3.4. Integration into displays and top-emitting devices

For the yield of a future display manufacturing process, an important benefit of the doping technique is the fact that rather thick doped transport layers can be used with still low operation voltages. We also find that the results are very reproducible using the doped transport layers because the performance becomes independent of the actual state and uniformity of the substrate surface.

Standard OLED structures emit through the substrate. However, for many applications, it would be useful if the emission were away from the substrate (top emitters). In principle, this can be achieved with a transparent cathode. However, on active-matrix substrates, cathode top emitters require the use of p-channel transistors for best operation, whereas inverted (anode on top) emitters work best with n-channel matrices. Anode on top devices also allow a fully transparent ITO cathode.

However, it has turned out to be difficult to realize efficient inverted top-emitting structures. The main reasons are that it is difficult to control the interface work functions for an inverted device. Accordingly, top-emitting structures showed much worse parameters than standard structures, in particular high operating voltages [46,47].

We have recently shown for the first time that the use of doped transport layers allow to realize highly efficient top-emitting structures [21] having an inverted top emitter structures deposited on ITO as cathode and using semitransparent gold as anode. Fig. 13 shows the current–voltage curves of

such device, realized on an ITO substrate and using a semitransparent gold contact. Both voltage and quantum efficiency are comparable to a substrate emitting device. The thick p-conducting top layer also allows the use of transparent oxide top contacts without significant damage to the OLED device [48]. These results are very promising for display applications, for instance in active-matrix OLED displays where efficient top emitter devices allow better use of the pixel area and where inverted devices allow the use of n-channel substrates. Furthermore, these results are useful for devices on fully opaque substrates, such as printed circuit board or metal foils.

4. Summary and outlook

In summary, we have discussed the controlled doping of organic semiconductors by coevaporation with suitable dopant molecules. The results show that the conductivities can be raised many orders of magnitude above the conductivity of nominally undoped materials. However, despite comparatively high doping ratios and high number of carriers generated, the achievable conductivities are still lower than in doped inorganic semiconductors due to the much lower mobilities of the organic semiconductors. Although the basic effects of doping like Fermi levels shifts can be well compared to the standard behavior of inorganic semiconductors, a detailed understanding of e.g. the dependence of conductivity on doping concentration requires models based on a subtle interplay of doping with localization and percolation effects. The n-type doping of organic semiconductors using molecular substances still needs improvement. A partial substitute can be the doping with alkali metals.

We further show that despite the rather low conductivities, doped organic semiconductors are well suited for device applications. For instance, for OLED, the conductivity is sufficient to avoid significant voltage drops even in thicker layers. Also, a key effect of doping, the generation of ohmic contacts by tunneling through a thin barrier formed by a space charge layers, works in organic semiconductors very well. This is in particular important for OLED devices where the undoped transport layers have required extensive measures to achieve low barrier at the interfaces and have made the devices very sensitive to the contact properties.

We have further shown that conductivity doped transport can significantly improve devices. For instance, we have achieved very low operating voltages for small-molecule devices; while the quantum efficiency is kept high. Also, we have first shown that doped transport layers allow realizing very efficient inverted top-emitting and transparent OLED devices.

Future work should address molecular n-type doping of OLED transport materials, avoiding the problems of alkali metal doping of the materials. Also, the doping concepts have not yet been systematically extended to OLED of all emission colors.

Acknowledgements

We thank S.R. Forrest (Princeton University: phosphorescent OLEDs) and N.R. Armstrong (University of Arizona: UPS/XPS measurements) for good and fruitful collaboration. We thank the German Secretary of Education and Science (BMBF) for financial support and Syntec GmbH, Wolfen, Germany for providing most of the used compounds.

References

[1] W.E. Spear, P.G. Le Comber, A.J. Snell, Philos. Mag. 38 (1978) 303.
[2] S.R. Forrest, Chem. Rev. 97 (6) (1997) 1793.
[3] N. Karl, in: Defect Control in Semiconductors, Vol. II, North Holland, Amsterdam, 1990.
[4] C.W. Tang, Appl. Phys. Lett. 48 (1986) 183.
[5] C.W. Tang, S.A.V. Slyke, Appl. Phys. Lett. 51 (1987) 913.
[6] Y. Yamamoto, K. Yoshino, Y. Inuishi, J. Phys. Soc. Jpn. 47 (1979) 1887.
[7] G. Parthasarathy, C. Shen, A. Kahn, S.R. Forrest, J. Appl. Phys. 89 (2001) 4986.
[8] J. Kido, T. Matsumoto, Appl. Phys. Lett. 73 (1998) 2866; J. Endo, T. Matsumoto, J. Kido, Jpn. J. Appl. Phys. Pt. 2 41 (3B) (2002) L358.

[9] D.R. Kearns, G. Tollin, M. Calvin, J. Chem. Phys. 32 (1960) 1020.
[10] M. Maitrot, G. Guillaud, B. Boudjema, J.J. André, J. Simon, J. Appl. Phys. 60 (1986) 2396.
[11] J.J. Andre, J. Simon, R. Even, B. Boudjema, G. Guillaud, M. Maitrot, Synth. Met. 18 (1987) 683.
[12] T.J. Marks, Science 227 (1985) 881.
[13] E.J. Lous, P.W.M. Blom, L.W. Molenkamp, D.M. deLeeuw, Phys. Rev. B 51 (1995) 17251.
[14] M. Pfeiffer, A. Beyer, T. Fritz, K. Leo, Appl. Phys. Lett. 73 (1998) 3202.
[15] M. Pfeiffer, T. Fritz, J. Blochwitz, A. Nollau, B. Plönnigs, A. Beyer, K. Leo, Adv. Solid State Phys. 39 (1999) 77.
[16] A. Nollau, M. Pfeiffer, T. Fritz, K. Leo, J. Appl. Phys. 87 (2000) 4340.
[17] B. Maennig, M. Pfeiffer, A. Nollau, X. Zhou, K. Leo, P. Simon, Phys. Rev. B 64 (2001) 195208.
[18] J. Blochwitz, M. Pfeiffer, T. Fritz, K. Leo, Appl. Phys. Lett. 73 (1998) 729.
[19] X. Zhou, M. Pfeiffer, J. Blochwitz, A. Werner, A. Nollau, T. Fritz, K. Leo, Appl. Phys. Lett. 78 (2001) 410.
[20] J.S. Huang, M. Pfeiffer, A. Werner, J. Blochwitz, K. Leo, S.Y. Liu, Appl. Phys. Lett. 80 (2002) 139.
[21] X. Zhou, M. Pfeiffer, J.S. Huang, J. Blochwitz-Nimoth, D.S. Qin, A. Werner, J. Drechsel, B. Maennig, K. Leo, Appl. Phys. Lett. 81 (2002) 922.
[22] J. Blochwitz, M. Pfeiffer, M. Hofman, K. Leo, Synth. Met. 127 (2002) 169.
[23] M. Pfeiffer, A. Beyer, B. Plönnigs, A. Nollau, T. Fritz, K. Leo, D. Schlettwein, S. Hiller, D. Wöhrle, Solar Energy Mater. Solar Cells 63 (2000) 83.
[24] D. Gebeyehu, B. Maennig, J. Drechsel, K. Leo, M. Pfeiffer, Solar Energy Mater. Solar Cells 79 (2003) 81.
[25] H. Fritzsche, Solid State Commun. 9 (1971) 1813.
[26] Y. Shirota, Y. Kuwabara, H. Inada, Appl. Phys. Lett. 65 (1994) 807.
[27] W. Gao, A. Kahn, Appl. Phys. Lett. 79 (2001) 4040.
[28] M. Yoshida, A. Fujii, Y. Ohmori, K. Yoshino, Appl. Phys. Lett. 69 (1996) 734.
[29] Y. Shirota, J. Mater. Chem. 10 (2000) 1.
[30] P.M. Borsenberger, J.J. Fitzgerald, J. Phys. Chem. 97 (1993) 4815.
[31] J. Kido, T. Matsumoto, Appl. Phys. Lett. 73 (1998) 2866.
[32] A.G. Werner, F. Li, K. Harada, M. Pfeiffer, T. Fritz, K. Leo, Appl. Phys. Lett. 82 (2003) 4495.
[33] T.A. Beierlein, W. Brutting, H. Riel, E.I. Haskal, P. Muller, W. Riess, Synth. Met. 111 (2000) 295.
[34] J. Drechsel, M. Pfeiffer, X. Zhou, A. Nollau, K. Leo, Synth. Met. 127 (2002) 201.
[35] C. Giebeler, H. Antoniadis, D.D.C. Bradley, Y. Shirota, J. Appl. Phys. 85 (1999) 608.
[36] J. Staudigel, M. Stoessel, F. Steuber, J. Simmerer, J. Appl. Phys. 86 (1999) 3895.
[37] B. Ruhstaller, S.A. Carter, S. Barth, H. Riel, W. Riess, J.C. Scott, J. Appl. Phys. 89 (2001) 4575.
[38] H. Aziz, Z.D. Popovic, N.-X. Hu, A.-M. Hor, G. Xu, Phys. Status Solidi A 283 (1999) 1900.
[39] Z.D. Popovic, H. Aziz, N.-X. Hu, A.-M. Hor, G. Xu, Synth. Met. 111–112 (2000) 229.
[40] M. Pfeiffer, S.R. Forrest, Unpublished results.
[41] S.E. Shaheen, B. Kippelen, N. Peyghambarian, J.F. Wang, J.D. Anderson, E.A. Mash, P.A. Lee, N.R. Armstrong, Y. Kawabe, J. Appl. Phys. 85 (1999) 7939.
[42] C.W. Tang, S.A. VanSlyke, C.H. Chen, J. Appl. Phys. 65 (1989) 3610.
[43] C.H. Chen, C.W. Tang, Appl. Phys. Lett. 79 (2001) 3711.
[44] X. Zhou, D.S. Qin, M. Pfeiffer, J. Blochwitz-Nimoth, A. Werner, J. Drechsel, B. Maennig, K. Leo, M. Bold, P. Erk, H. Hartmann, Appl. Phys. Lett. 81 (2002) 4070.
[45] M. Pfeiffer, S.R. Forrest, M.E. Thompson, K. Leo, Adv. Mater. 14 (2002) 1633.
[46] V. Bulovic, P. Tian, P.E. Burrows, M.R. Gokhale, S.R. Forrest, M.E. Thompson, Appl. Phys. Lett. 70 (1997) 2954.
[47] G. Parthasarathy, P.E. Burrows, V. Khalfin, V.G. Kozlov, S.R. Forrest, Appl. Phys. Lett. 72 (1998) 2138.
[48] M. Pfeiffer, S.R. Forrest, X. Zhou, K. Leo, Org. Electron. 4 (2003) 21.
[49] J. Blochwitz, M. Pfeiffer, T. Fritz, K. Leo, D.M. Alloway, P.A. Lee, N.R. Armstrong, Org. Electron. 2 (2001) 97.
[50] C. Adachi, R. Kwong, S.R. Forrest, Org. Electron. 2 (2001) 37.